**Atmospheric
Chemistry
and Physics
Discussions**

**Hohenpeissenberg
Aerosol
Characterization
Experiment 2002**

N. Hock et al.

# Rural continental aerosol properties and processes observed during the Hohenpeissenberg Aerosol Characterization Experiment (HAZE2002)

**N. Hock[1], J. Schneider[1], S. Borrmann[1,2], A. Römpp[3,*], G. Moortgat[3], T. Franze[4], C. Schauer[4], U. Pöschl[4,**], C. Plass-Dülmer[5], and H. Berresheim[5,***]**

[1]Particle Chemistry Dept., Max Planck Institute for Chemistry, Mainz, Germany
[2]Institute for Atmospheric Physics, Johannes Gutenberg University, Mainz, Germany
[3]Atmospheric Chemistry Dept., Max Planck Institute for Chemistry, Mainz, Germany
[4]Institute of Hydrochemistry, Technical University of Munich, Germany
[5]German National Meteorological Service (DWD), Observatory Hohenpeissenberg, Germany
[*]now at: Institute for Inorganic and Analytical Chemistry, Justus Liebig University Giessen, Germany
[**]now at Biogeochemistry Dept., Max Planck Institute for Chemistry, Mainz, Germany
[***]now at: Dept. of Physics, National University of Ireland, Galway, Ireland

Correspondence to: J. Schneider (schneider@mpch-mainz.mpg.de)

Title Page

| Abstract | Introduction |
| Conclusions | References |
| Tables | Figures |

|◄ | ►|

◄ | ►

Back | Close

Full Screen / Esc

Printer-friendly Version

Interactive Discussion

EGU

**Hohenpeissenberg Aerosol Characterization Experiment 2002**

N. Hock et al.

**Abstract**

Detailed investigations of the chemical and microphysical properties of rural continental aerosols were performed during the HAZE2002 experiment, which was conducted in May 2002 at the Meteorological Observatory Hohenpeissenberg (DWD) in Southern
5 Germany.

The online measurement data and techniques included: size-resolved chemical composition of submicron particles by aerosol mass spectrometry (AMS); total particle number concentrations and size distributions over the diameter range of 3 nm to 9 $\mu$m (CPC, SMPS, OPC); monoterpenes determined by gas chromatography- ion trap
10 mass spectrometry; OH and $H_2SO_4$ determined by atmospheric pressure chemical ionization mass spectrometry (CIMS). Filter sampling and offline analytical techniques were used to determine: fine particle mass (PM2.5), organic, elemental and total carbon in PM2.5 (OC2.5, EC2.5, TC2.5), and selected organic compounds (dicarboxylic acids, polycyclic aromatic hydrocarbons, proteins).
15 Overall, the non-refractory components of submicron particles detected by aerosol mass spectrometry (PM1, 6.6±5.4 $\mu$g m$^{-3}$, arithmetic mean and standard deviation) accounted for ~62% of PM2.5 determined by filter gravimetry (10.6±4.7 $\mu$g m$^{-3}$). The relative proportions of non-refractory submicron particle components were: 11% ammonium, 19% nitrate, 20% sulfate, and 50% organics (OM1). In spite of strongly
20 changing meteorological conditions and absolute concentration levels of particulate matter (3–13 $\mu$g m$^{-3}$ PM1), OM1 was closely correlated with PM1 (r$^2$=0.9) indicating a near-constant ratio of non-refractory organics and inorganics. In contrast, the ratio of nitrate to sulfate was highly dependent on temperature (14–32°C) and relative humidity (20–100%), which could be explained by thermodynamic model calculations
25 of $NH_3/HNO_3/NH_4NO_3$ gas-particle partitioning. From the combination of optical and other sizing techniques (OPC, AMS, SMPS), an average refractive index of 1.40–1.45 was inferred for the measured rural aerosol particles.

The average ratio of OM1 to OC2.5 was 2, indicating a high proportion of heteroele-

ments in the organic fraction of the sampled rural aerosol. This is consistent with the high ratio of oxygenated organic aerosol (OOA) over hydrocarbon-like organic aerosol (HOA) inferred from the AMS results (4:1), and also with the high abundance of proteins (∼3%) indicating a high proportion of primary biological material (∼30%) in PM2.5.

5 Moreover, the low abundance of PAHs ($<1\,\mathrm{ng\,m^{-3}}$) and EC ($<1\,\mu\mathrm{g\,m^{-3}}$) in PM2.5 confirm a low contribution of combustion emissions, which are usually also major sources for HOA. Slightly enhanced HOA concentrations indicating fresh anthropogenic emissions were observed during a period when air masses were advected from the densely populated Po Valley, Italy.

10 Detection of several secondary organic aerosol compounds (dicarboxylic acids) and their precursors (monoterpenes) confirmed the finding that secondary aerosol from natural sources was an important aerosol constituent. A sharp decrease of the short lived monoterpenes indicated that during night-time the measurement station was isolated from ground emission sources by a stable inversion layer. Nighttime values can

15 therefore be regarded to represent regional or long range transport.

New particle formation was observed almost every day with particle number concentrations exceeding $10^4\,\mathrm{cm^{-3}}$ (nighttime background level 1000–2000 $\mathrm{cm^{-3}}$). Closer inspection of two major events indicated that ternary $H_2SO_4/H_2O/NH_3$ nucleation triggered particle formation and that condensation of both organic and inorganic species

20 contributed to particle growth.


## 1  Introduction

Aerosol particles represent an important constituent of the Earth's atmosphere, since they influence the radiative balance, the chemical composition and the water cycle of the atmosphere. The radiative effects include the direct aerosol effects, i.e. the direct

25 backscattering of incoming solar radiation into space, and the indirect effects due to the ability of aerosol particles to act as CCN (cloud condensation nuclei) and thereby to alter cloud properties (Lohmann and Feichter, 2005). Furthermore, aerosol particles

affect air quality and human health. Several studies showed a direct link between adverse effects on human health and fine particle ($d < 2.5\,\mu m$) as well as ultrafine particles ($d < 0.1\,\mu m$) (Oberdorster, 2001; Pope et al., 2002; Pope and Dockery, 2006).

A significant fraction of atmospheric aerosol particles are formed by gas-to-particle
5   conversion (nucleation) of sulfuric acid, ammonia, water, and/or oxidized hydrocarbons (see review articles by (Kulmala et al., 2004) and (Curtius, 2006). The mentioned precursor compounds can be of anthropogenic or natural origin. While sulfuric acid has been identified in several experiments to trigger atmospheric nucleation (Berndt et al., 2005; Birmili et al., 2003; Birmili et al., 2000), the role of organic compounds is an
10  open question (Bonn and Moortgat, 2002, 2003; Curtius, 2006).

The chemistry of atmospheric aerosols, especially their organic chemistry, is very complex, and the investigation of aerosol formation and atmospheric transformation processes is an ongoing challenge (Fuzzi et al., 2006; Poschl, 2005; Rogge et al., 1998; Seinfeld and Pankow, 2003). The above mentioned effects of aerosol particles
15  on health, clouds, and climate depend both on the size (a physical property) and on the chemical composition of the aerosol particles. A recent study by (Dusek et al., 2006) suggested that size matters more than chemistry in CCN activation of aerosol particles, but this issue is currently under debate.

To achieve a better understanding of these atmospheric aerosol processes, it is es-
20  sential to have size-resolved information on the chemical composition of the aerosol phase, besides many other aerosol properties. The large experimental setup that is needed to characterize the ambient aerosol can only be realized within intensive field studies. Such an intensive aerosol study, the Hohenpeissenberg Aerosol Characterization Experiment (HAZE), was performed in May 2002 at the Meteorological Obser-
25  vatory Hohenpeissenberg (MOHp). The objective of this campaign was to perform a detailed study on physical and chemical properties of continental rural aerosol particles. The MOHp is located at a rural site about 40 km north of the Alps and surrounded by forest and agricultural pastures. In previous long-term measurements at MOHp the formation of new particles from gaseous precursors (in particular $H_2SO_4$) was ob-

served quite frequently during spring but only rarely in summer (Birmili et al., 2000, 2003).

In the present paper we report on the results of the HAZE2002 study with respect to the chemical composition and size distribution of the aerosol phase, with emphasis on the organic composition inferred from mass spectrometry and filter analyses, comparison of the methods, mass closure, and the dependence of the aerosol properties on meteorological conditions as temperature and air mass origin.

## 2  Experimental

The HAZE2002 Experiment was conducted between 16 May 2002 and 30 May 2002 at the Meteorological Observatory Hohenpeissenberg (47°48′ N, 11°02′ E, 985 m a.s.l.) which is operated by Deutscher Wetterdienst (DWD) and is part of the WMO GAW program. The observatory is located at about 300 m elevation above the surrounding area in a region with significant agricultural structure. A broad range of meteorological, trace gas, and aerosol parameters is continuously measured at MOHp, among which are $H_2SO_4$ and OH, measured by selected ion chemical ionization mass spectrometry (SI/CIMS) (Berresheim et al., 2000), number density of aerosol particles with $d>3$ nm and $d>14$ nm using condensation particle counters (CPC, models 3025A and 7610, TSI Inc., St. Paul, Minnesota) as well as monoterpenes and aromatic hydrocarbons which are monitored using gas chromatography – ion trap mass spectrometry (Birmili et al., 2003).

During the HAZE2002 campaign the following additional measurements were performed: The size distribution of ambient aerosol particles was measured with an optical particle counter (OPC PALAS model PCS 2010) for particles with diameters between 270 nm and 9.5 $\mu$m, and with a scanning mobility particle sizer (SMPS, models 3081 and 3085, TSI Inc.) for particle size ranges 7–300 mn and 3–65 nm, respectively. The number density of aerosol particles with $d>3$ nm has been measured with an ultra-fine condensation particle counter (UCPC, model 3025A, TSI Inc.). The size-resolved

chemical composition of non-refractory submicron aerosol particles was measured with the Aerodyne Q-AMS (Quadrupole Aerosol Mass Spectrometer) (Allan et al., 2003; Canagaratna et al., 2007; Jayne et al., 2000; Jimenez et al., 2003b). Q-AMS mass concentration and size distribution data were taken between 20 May 2002 and 30 May 2002, with a time resolution of 6 min. For the calculation of ambient mass concentrations, a collection efficiency with respect to particle bounce from the vaporizer (*CE*) of 0.5 was used (Alfarra et al., 2004; Allan et al., 2004). Implications and errors that result from this assumption will be discussed in the following sections. The aerodynamic lens of the Q-AMS (Zhang et al., 2002; Zhang et al., 2004) transmits particles in the size range (vacuum aerodynamic diameter, $d_{va}$) from 50 to 600 nm with 100% efficiency. The transmission of the lens drops off significantly for $d_{va} > 1\,\mu$m, providing similar characteristics to PM1 size selective inlets used in filter based measurements (Weimer et al., 2006).

Filter samples of fine air particulate matter (PM2.5) were collected on 150 mm diameter glass fiber filters (Macherey-Nagel, MN 85/90 binder-free) with a high volume filter sampler (HVS; Digitel DHA 80, volumetric flow rate 500 L/min, sampling interval 24 h). Prior to use, the filters were heated to 300°C for 12–18 h in a muffle furnace to remove organic contaminants. For gravimetric mass determination of the sampled particulate matter, the filters were conditioned at 45% relative humidity at room temperature (295 K) over saturated $K_2CO_3$-solution in a glass desiccator for 2 days before weighing. After weighing on an analytical balance, the samples were wrapped in aluminium foil and stored at –20°C. The total carbon (TC2.5) and elemental carbon (EC2.5) contents of the aerosol filter samples have been determined with a thermochemical carbon analyzer (Stroehlein Coulomat 702). TC2.5 was measured by combustion of sample aliquots under $O_2$ at 600°C and detection of the evolved $CO_2$ by coulometric detection. For EC determination the sample aliquots were pre-conditioned by solvent extraction and thermal desorption prior to combustion; organic carbon (OC2.5) was determined as the difference between TC2.5 and EC2.5 (Schauer et al., 2004). Polycyclic aromatic hydrocarbons (PAH) were determined by high performance liquid chro-

matography with fluorescence detection (Schauer et al., 2004, 2003a; Schauer et al., 2003b). The PAH concentrations reported in this manuscript refer to the sum of 12 out of the 16 EPA PAH priority pollutants: phenanthrene, anthracene, fluoranthene, pyrene, benzo[a]anthracene, chrysene, benzo[b]fluoranthene, benzo[k]fluoranthene, benzo[a]pyrene, dibenz[ah]anthracene, benzo[ghi]perylene, indeno[1,2,3-cd]pyrene. Not included are the four EPA PAHs with lowest molecular mass and highest volatility (naphthalene, acenaphthene, acenaphthylene, fluorine).

Proteins were determined with a bicinchoninic acid assay calibrated with bovine serum albumin (Franze, 2004; Franze et al., 2005). The reported values have to be considered as equivalent concentrations which approximate the actual protein content of the samples but may be influenced by related macromolecular substances – e.g., humic or humic-like substances, respectively (Fehrenbach, 2006; Franze, 2004; Ivleva et al., 2007).

On 22 May 2002 and 23 May 2002, filter samples were taken with a time resolution of 3 h during the day (08:00 to 20:00) and 12 h during the night (20:00 to 08:00 CEST) using an additional Digitel DA-80 high volume sampler, also equipped with a 2.5 $\mu$m sampling head (calculated for a volumetric sample flow rate of 500 L min$^{-1}$). The flow rate in this study was increased to 1000 L min$^{-1}$ resulting in a cut-off size of 2.0 $\mu$m. The samples were analyzed for carboxylic acids with a LC/MS/MS-ToF instrument combining tandem mass spectrometry and high mass resolution measurements (Römpp, 2003). A regular reversed-phase HPLC system (2 mm C$_{18}$ colum) was coupled to a hybrid mass spectrometer (quadrupole and time-of-flight) QSTAR (Applied Biosystems MDS SCIEX, Toronto, Canada) by an electrospray ion source.

The Q-AMS as well as the SMPS, OPC and UCPC were set up in a laboratory in the top floor of the observatory on the southwestern side facing the dominant wind direction. The aerosol samplers were mounted outside on the roof platform of the building, and precautions were taken that the exhaust of the instrument did not affect the particle sampling. The particle inlet to the indoor instruments, a stainless steel tube with a length of 2 m and an inner diameter of 8 mm, was designed to be near-isokinetic.

Raindrops were prevented from entering the line by means of a downward facing funnel at the beginning of the line. The tube included one 90°-bend to transmit the particles to the Q-AMS as well as to the SMPS, UCPC and OPC. Ambient air was pumped through this tube with $25 \, L \, min^{-1}$, including a sample flow of $0.1 \, L \, min^{-1}$ of the Q-AMS. The transport losses of the sampling system with respect to inertia, diffusion and settling losses have been calculated based on simple aerodynamic calculations (Hinds, 1999). Averaged over the size ranges that are detected by the Q-AMS, the SMPS, the UCPC, and the OPC the total transport losses are smaller than 12%.

## 3  Results and discussion

### 3.1  Overview and aerosol mass closure

Figure 1 gives an overview on the time series of several important parameters measured during the HAZE2002 project: Panel a) shows the time series temperature and relative humidity. Panel b) gives the number density for particles larger than 3 nm and for particles with diameters between 3 and 14 nm (ultrafine particles), along with time series of the $H_2SO_4$ concentration. Panel c) shows the number size distribution measured with the SMPS. Panel d) gives the time series of the mass concentrations of the major species sulfate, nitrate, ammonium and organics measured with the Q-AMS. Panel e) shows the individual chemical compounds ($NO_3$, $SO_4$, $NH_4$, Organics from the Q-AMS, EC2.5 from the HVS), averaged corresponding to the HVS averaging times and stacked onto each other, along with the PM2.5 total mass concentration and the OC from the HVS (OC2.5).

Panels a) to c) reveal that the temperature, the number concentration of total and ultrafine particles, and $H_2SO_4$ number concentration show a pronounced diurnal cycle, which is an indication for photochemical particle formation. This will be discussed in more detail in Sect. 3.5.

The mass concentrations measured with the Q-AMS data (Panels d and e) show

a large variation, ranging between $3\,\mu g/m^3$ to $13\,\mu g/m^3$ (diurnal averaged concentration). All four species increase significantly between 21 May 2002 and 23 May 2002 with values for both nitrate and organics reaching up to $14\,\mu g/m^3$. Also the sulfate and ammonium mass concentrations during this period markedly exceed the average
5  values measured during the campaign. Backward trajectory calculations performed with the LM1 model of DWD and with the NOAA HYSPLIT model confirmed that the air masses that arrived at the Hohenpeissenberg station between 21 May 2002, 22:00, and 23 May 2002, 20:00, have encountered the polluted Po Valley area in northern Italy within the planetary boundary layer between 18 and 48 h prior to our measurements.
10 The arrival times of the trajectories originating from the Po Valley are indicated with the horizontal bar in panel d) of Fig. 1.

   The correlation between PM1 and the HVS mass concentration (PM2.5) is given in Fig. 2a). To obtain PM1, we added EC2.5 to the sum of the Q-AMS concentrations to account for the fact that the Q-AMS does not detect elemental carbon. The error
15 by adding a PM2.5 quantity to PM1 data is regarded to be negligible, since firstly, we do not expect a large fraction of elemental carbon to be found in the size range between 1.0 and $2.5\,\mu m$ and secondly, the amount of EC is small compared to the non-refractory mass concentrations. The term "PM1" in this paper will therefore refer to "sum Q-AMS" plus EC2.5. The linear regression has a slope of 0.68. The overall
20 ratio of PM1 to PM2.5 was 0.62. Note that other refractory material like mineral dust is also not measured by the Q-AMS. It further has to be noted that the ratio PM1 to PM2.5 is directly dependent on the chosen *CE* factor of the Q-AMS which, as explained above, was set to 0.5 for all species.

   Chemical resolved mass concentrations from the HVS sampler are available only for
25 organic carbon (OC2.5), which is calculated by the difference of total carbon (TC2.5) and elemental carbon (EC2.5). Figure 2b shows the correlation between the total organic mass concentration measured with the Q-AMS (= total organic matter, OM1) and OC2.5. Although large variations of the total aerosol concentration and composition have been observed during the campaign, both data sets are well correlated

with an $r^2$ value of 0.63. The linear regression slope between OM1 and OC2.5 is 2.07, which is at the upper end of the approximated OM/OC ratios reported by (Lim and Turpin, 2002; Turpin and Lim, 2001) of 1.6 for urban organic aerosol and of 2.1 for aged organic aerosol, and indicates that the average organics aerosol measured
5  during HAZE was substantially photochemically processed. It must be stressed that this ratio is directly dependent on the assumed Q-AMS collection efficiency factor for organic particles which was chosen to $CE$ = 0.5. But since the same conclusion will later be drawn from a Q-AMS internal method (independent on $CE$, see Sect. 3.4), the picture is consistent.
10  Figure 2c shows the correlation between total carbon (TC2.5) and total particulate matter (PM2.5), Fig. 2d) gives the correlations between OC2.5 and PM2.5 as well as between OM1 and PM1. The high correlation between OM1 and PM1 ($r^2$=0.90) indicates that in spite of strongly changing meteorological conditions and absolute concentration levels of particulate matter (3–13 $\mu$g m$^{-3}$ PM1), the ratio of non-refractory
15  organics and inorganics of 1:1 was nearly constant.

3.2  Aerosol size distributions

Figure 3 gives the chemically resolved size distributions of the 4 species measured by the Q-AMS as a function of time for the second week of the campaign. In the following we will concentrate on three time periods A, B, and C (see Table 1 and Fig. 3) show-
20  ing a distinct difference in the chemically resolved size distributions. Figure 4 depicts the size distributions averaged for these three time periods A, B, and C. Size distribution data have additionally been obtained from SMPS and OPC. In order to compare the size distributions obtained with Q-AMS, SMPS, and OPC, the mean density of the aerosol particles was estimated from the chemical composition. Ammonium sulfate
25  and ammonium nitrate were calculated from the measured sulfate and nitrate content. These data are given in Table 1. The vacuum aerodynamic diameter ($d_{va}$) was converted into volume equivalent diameter $d_{ve}$ under the assumption of spherical particles

using the equation

$$d_{ve} = d_{va} \cdot \frac{\rho_0}{\rho_p} \qquad (1)$$

(Jimenez et al., 2003a), where $\rho_p$ is the particle density and $\rho_0$ is the density of water. The mobility diameter measured by the SMPS equals the volume equivalent diameter for spherical particles (DeCarlo et al., 2004).

For the optical particle counter PALAS PCS 2010, we performed Mie calculations following the algorithms of (Bohren and Huffmann, 1983), in order to find the refractive index at which the obtained size distributions match best to the AMS size distribution. The PCS 2010 operates with a white light source and the scattered light is detected under 90° (Umhauer, 1983). It was calibrated with PSL spheres of 800 nm (refractive index $n$=1.588) at the beginning of the campaign. By comparing the total mass distribution of the Q-AMS and the mass distribution obtained by the OPC (using the density inferred from chemical composition), it was found that the data match best for refractive indices of 1.400 and 1.450, respectively (see Table 1). The SMPS size range reaches only up to 65 nm (due to the use of the Nano-DMA). In this size range the transmission of the aerodynamic lens of the Q-AMS is less than 100%. Additionally, the low mass concentrations observed in period C leads to larger uncertainties and therefore also to some negative values in the mass size distributions measured by the Q-AMS, which makes comparison between Q-AMS and SMPS difficult, although qualitative agreement is achieved.

In the following we will focus on the wet removal process observed during a precipitation event which occurred between 14:00 and 20:00 on 25 May 2002, with highest rain rates of $>0.1 \, \text{L} \, \text{m}^{-2} \, \text{min}^{-1}$ between 14:00 and 16:00 (lowest panel of Fig. 3). These three time periods reflect the wet removal of aerosol particles during the precipitation event on 25 May 2002. The CO data (lowest panel of Fig. 3) show that no air mass change occurred during the precipitation event and therefore the decrease of the mass concentrations (Table 1) is only due to wet removal. The mass concentrations before and after the precipitation event suggest different wet removal efficiency for the different

Title Page

Abstract | Introduction

Conclusions | References

Tables | Figures

|◄ | ►|

◄ | ►

Back | Close

Full Screen / Esc

Printer-friendly Version

Interactive Discussion

EGU

species: Ammonium sulfate is removed by a factor of 12, ammonium nitrate by a factor of 19, organics by a factor of 8.

This can be seen as an indication for partial external mixture of the aerosol particles, since in a complete internal mixture all species would be removed to the same degree. Small organic particles appear to be less efficiently removed, as shown by panel C: After the precipitation event, an aerosol mode around 60–80 nm is present which is dominated by organic compounds.

## 3.3 Temperature dependence of ammonium nitrate in the aerosol phase

Ammonium nitrate ($NH_4NO_3$) is one of the major components of the particulate matter measured during HAZE2002. The ambient temperature during HAZE2002 was highly variable, ranging between 32°C and 14°C (see Fig. 1). On days with higher ambient temperature the relative ammonium nitrate content in the aerosol particles was observed to be lower than on colder days. Previously published data by several authors (Willison et al., 1985) demonstrate that the nitrate concentration in the fine particle mode has a wintertime maximum and summertime minimum in correspondence with temperatures. It is also indicated that in summer gas phase nitrate has a greater concentration than particulate nitrate, while in winter the opposite situation can be observed (Meszaros and Horvath, 1984; Morino et al., 2006). Observations by (Seidl et al., 1996) show a direct relationship between the ratio of gaseous nitrate to fine particulate nitrate and temperature. They conclude that above a limit of 15–20 C most of the nitrate is in gas phase, while below this temperature range nitrate can be detected in aerosol form. The observed connection between temperature and the amount of ammonium nitrate on the aerosol phase during HAZE2002 is investigated here in more detail:

Ammonium nitrate is formed by the reaction of gaseous ammonia ($NH_3^{(g)}$) and nitric acid ($HNO_3^{(g)}$):

$$HNO_3^{(g)} + NH_3^{(g)} \leftrightarrow NH_4NO_3^{(a)} \tag{2}$$

Here ($g$) indicates a gas phase compound and ($a$) a compound in the aerosol phase. If the ambient relative humidity (RH) is lower than the deliquescence relative humidity (DRH), ammonium nitrate exists in the solid phase, if RH is higher than DRH, $NH_4NO_3$ dissociates to $NH_4^+$ and $NO_3^-$ in an aqueous solution. If $NH_3$ and $HNO_3$ can exchange readily between the gas and particle phases, an equilibrium exists between atmospheric $NH_4NO_3^{(a)}$, $NH_3^{(g)}$ and $HNO_3^{(g)}$ (Mozurkewich, 1993) and the gas-phase concentration of $NH_3^{(g)}$ and $HNO_3^{(g)}$ is determined by this equilibrium. Furthermore, the rate of evaporation of $NH_4NO_3^{(a)}$ from particles depends on its dissociation constant $K$.

The deliquescence relative humidity can be parameterized as a function of temperature:

$$\ln(\text{DRH}) = \frac{723.7}{T} + 1.6954 \tag{3}$$

where $T$ is the ambient temperature in Kelvin and DRH is given in % (Seinfeld and Pandis, 1998). Under the condition that RH<DRH, the $NH_4NO_3$ dissociation constant $K_{\text{NH4NO3}}$ equals $p_{\text{HNO3}} \cdot p_{\text{NH3}}$, where $p_{\text{HNO3}}$ and $p_{\text{NH3}}$ are the equilibrium partial pressures of $HNO_3$ and $NH_3$ in the gas phase. The dependence of $K$ on the temperature $T$ is given the by following parameterization (Stelson and Seinfeld, 1982):

$$\ln K(T) = 84.6 - \frac{24220}{T} - 6.1 \cdot \ln\left(\frac{T}{298}\right) \tag{4}$$

where $K$ is in units of $\text{ppb}^2$ and $T$ in Kelvin. Lower temperatures correspond to lower values of $K$ and therefore to lower equilibrium values of $NH_3^{(g)}$ and $HNO_3^{(g)}$. Hence lower temperatures shift the equilibrium of the system towards the aerosol phase, increasing the aerosol mass of $NH_4NO_3$. Additionally, it has to be considered that the available sulfate will react primarily with $NH_4$ and only the excess $NH_4$ is available for $NH_4NO_3$ formation. The resulting equation for the calculation of the molar concentra-

tion of ammonium nitrate [NH$_4$NO$_3^{(a)}$] is, following (Seinfeld and Pandis, 1998):

$$\left[NH_4NO_3^{(a)}\right] = \frac{\left([TA]-2\left[SO_4^{2-}\right]+[TN]\right)}{2} + \left(\frac{\left([TA]-2\left[SO_4^{2-}\right]+[TN]\right)^2}{4} - [TN]\left([TA]-2\left[SO_4^{2-}\right]\right)-K\right)^{\frac{1}{2}} \quad (5)$$

with:

$$[TA] = \left[NH_3^{(g)}\right] + \left[NH_4^+\right]$$
$$[TN] = \left[HNO_3^{(g)}\right] + \left[NO_3^-\right]$$

5     where the total molar concentration of ammonia [$TA$] is the sum of molar concentration of ammonia in the gas phase [$NH_3^{(g)}$] and the molar concentration of ammonium in the aerosol phase [$NH_4^+$]. Similarly, the total nitrate concentration [$TN$] is the sum of the nitric acid concentration in the gas phase and the nitrate concentration in the aerosol phase. The available ammonia for reaction with nitric acid is therefore [TA] − 2[$SO_4^-$]

10  since every mole sulfate has removed 2 moles ammonia from the gas phase.

    Equation (5) is only valid for the case that ammonium nitrate in the aerosol phase is solid, a condition that is usually not fulfilled in the atmosphere. The hysteresis effect of the deliquescence curve leads to the presence of dissolved ammonium nitrate when RH<DRH, since efflorescence (or crystallization) occurs at markedly lower RH

15  values than the deliquescence. However, calculation of the equilibrium gas-particulate partitioning of ammonium nitrate for RH>DRH requires a more complicated, numerical model calculation (Seinfeld and Pandis, 1998) that is beyond the scope of this paper.

    Figure 5 shows the ratio of ammonium nitrate mass concentration and the total non-refractory PM1 mass concentration (measured with the Q-AMS), as a function of tem-

20  perature. The ammonium nitrate mass concentration was calculated as follows:

$$[NH_4NO_3] = [NO_3]_{meas} + [NH_4]_{meas} - 2 \times [SO_4]_{meas} \times M_{NH4}/M_{SO4} \quad (6)$$

where the last term accounts for the ammonia neutralized by sulfate. The dots represent 2h-mean values, the blue crosses give the values binned into temperature bins of

EGU

2 K below 298 K. Above 298 K we used one 4-K bin and one 5-K bin, since less data points were available.

The solid line represents the calculated ratio of $NH_4NO_3^{(a)}$ to total $PM_1$, following Eq. (5). [$TA$] was parameterized as [$TA$]=$a$+exp($b \times (T-c)$) (in pbb), increasing with temperature as observed/predicted by (Allen et al., 1988) and (Krupa, 2003). The curve was fitted to the experimental values using $a$, $b$, $c$, and [$TN$] as free parameters. The fitting routing yielded: [$TN$]=0.951 ppb and [$TA$] ranging between 1 and 2.8 ppb ($a$=0.977, $b$=0.295, $c$=301 K). The displayed curve represents the best fit to the data under the given conditions. The results of the fit imply a gas phase concentration of $HNO_3$ of less then 1 ppb, which is on the lower side of previously published observations, e.g., (Cadle et al., 1982; Finlayson-Pitts and Pitts, 1986; Morino et al., 2006) and a total ammonia concentration between 1 and 2.8 ppb in the observed temperature range, which is lower than the values observed by (Morino et al., 2006) over Tokyo, ranging between 5 and 10 ppbv in summer.

The model curve represents qualitatively the measured values, although it corresponds better to the maximum measured values at a given temperature than the mean values. The reason is most likely the above mentioned fact that the calculation is only valid for solid ammonium nitrate that is not deliquesced. However, with this simple conceptual model it was possible to qualitatively reproduce the observed ammonium nitrate in the aerosol phase with the measured input parameters aerosol sulfate and temperature. The necessary assumption concerning the parameterization of the total ammonia concentration is not unrealistic. However, it would be of great benefit to have gas phase ammonia and nitric acid measurements for future aerosol studies in the rural continental atmosphere.

## 3.4 The organic fraction of the aerosol particles

### 3.4.1 Oxygenated organic aerosol (OOA) and hydrocarbon-line organic aerosol (HOA)

The correlation between the organic mass concentration measured by the Q-AMS (OM1) and OC2.5 measured by the HVS (Fig. 2b) has already been discussed (Sect. 3.1). In Fig. 6 the diurnal pattern of the total organic mass concentration, measured by the AMS, and the mass concentrations of $m/z$ 44 and $m/z$ 57 are shown. In the AMS, $m/z$ 44 is an indicator for oxygenated organic aerosol (OOA), while $m/z$ 57 is indicator for hydrocarbon-like organic aerosol (HOA) (Zhang et al., 2005a; Zhang et al., 2005c). HOA is usually associated with fresh anthropogenic emissions, as diesel exhaust. The dots represent the averages of the measured mass concentrations within one hour. The boxes are the 25th percentile, the median and the 75th percentile; the "whiskers" below and above represent the 5th and 95th percentiles of the averaged data. The diurnal pattern of the total organics seems to be dominated by the distinct diurnal pattern of $m/z$ 44 with a maximum between 14:00 and 17:00, while the diurnal pattern of $m/z$ 57 is much less pronounced. This indicates that the oxidized organic compounds measured during the HAZE2002 campaign were produced by photochemical conversion during daylight hours, most likely from biogenic precursor emissions. During new particle formation events, these photochemically formed oxidized organics compounds may contribute significantly to the growth of the newly formed particles. Direct emissions of hydrocarbon-like aerosol (e.g. traffic exhaust), play only a minor role in he diurnal cycle, especially the morning traffic peak between 07:00 and 09:00 is missing. This morning traffic peak has been observed previously in urban measurements (Drewnick et al., 2004; Zhang et al., 2005b) where primary anthropogenic HOA emissions are more important. Using the algorithm of Zhang et al. (2005a), the overall ratio of OOA to HOA was found to be 4:1 (Zhang et al., 2007).

Figure 7 shows the correlation between the mass concentration of $m/z$ 44 and the total organic mass concentration for the measurements during HAZE2002. The data

points reveal an average regression slope of 0.09 for the HAZE2002 data. For comparison, the slopes from two other data sets are plotted: Data obtained from diesel exhaust particles that contain mainly hydrocarbon-like organic compounds yield a slope of 0.05 (Schneider et al., 2006), while data measured in the free troposphere at the research station Jungfraujoch (Switzerland) during the CLACE 3 campaign (March 2004, Walter et al., 2007[1]) are highly oxidized and reveal a slope of 0.20. This implies that the organic compounds in the aerosol particles measured during HAZE2002 are oxidized to a lesser degree than aerosol observed in the free troposphere, and that the ratio of m/z 44 to total organics measured with the Q-AMS can be used as an approximation for the degree of oxidation of organic aerosol compounds for ambient aerosol data. This method has already been applied by (Takegawa et al., 2005) for Tokyo city, who inferred a low degree of oxidation for a ratio of m/z 44 to total organics below 0.04 and a highly oxidized aerosol for a ratio above 0.08. Following this classification, the average aerosol observed during HAZE2002 was "highly" oxidized. However, it must be stressed that this method can only be applied in field data that are not influenced be fresh biomass burning emissions since biomass burning particles are likely to deviate from this behavior (Schneider et al., 2006). A highly oxidized aerosol can be an indicator for processed, aged aerosol, but also for aerosol formed from oxidized biogenic precursors. Also given in Fig. 7 is the slope of the part of the data when the air masses arrived from the Po Valley, Italy, and the organic mass concentrations were highest (21 May 2002, 22:00–23 May 2002, 20:00, labelled "polluted"). For these data, the slope is slightly lower (0.08), indicating a less oxidized aerosol.

Figure 8 illustrates this diagnostic by comparing different organic aerosol mass spectra: a) a mass spectrum averaged for the period when the air masses arrived from the Po Valley (21 May 2002, 22:00–23 May 2002, 20:00) with b) a mass spectrum averaged

---

[1]Walter, S., S., Schneider, J., Hock, B. N., Curtius, J., Borrmann, S., Mertes, S., Weingartner, E., Verheggen, B., Cozic J., J. Baltensperger J., Allan J. D., Crosier, J., Bower, K., and Coe, H.: On the chemical composition of ice nuclei: Results from the 3rd and 4th Cloud and Aerosol Characterization Experiment (CLACE), Atmos. Chem. Phys. Discuss., in preparation, 2007.

Title Page

Abstract | Introduction

Conclusions | References

Tables | Figures

◀ | ▶

◀ | ▶

Back | Close

Full Screen / Esc

Printer-friendly Version

Interactive Discussion

EGU

over an episode when the air masses arrived from the west (24 May 2002, 00:00–24 May 2002, 12:00); c) a mass spectrum of free tropospheric aerosol sampled at the High Alpine Research Station Jungfraujoch during the CLACE-3 project (Walter et al., 2007[1]; and d) a mass spectrum from diesel engine exhaust particles measured on a
5   engine test dynamometer (Schneider et al., 2006). Only the organic signals are shown.

In the mass spectrum a), the mass fragments $m/z$ 43 ($C_3H_7^+$ or $C_2H_3O^+$) and 44 ($CO_2^+$) have the biggest contribution to the organic compounds, followed by $m/z$ 55 ($C_4H_7^+$ or $C_3H_3O^+$). Similar to $m/z$ 44, $m/z$ 18 ($H_2O^+$) is also a fragmentation product of the vaporization of oxidized aerosol compounds and has found to be equal in size as
10   $m/z$ 44 (Alfarra et al., 2004). In the mass spectrum a) the relative contributions of $m/z$ 43 and $m/z$ 44 are almost equal in size, whereas in mass spectrum b) m/z 44 exceeds m/z 43. Panels c) and d) show the extreme cases, analog to the lines in Fig. 7: in aged organic aerosol (as encountered in the free troposphere) $m/z$ 44 dominates, while in fresh anthropogenic emissions (as in diesel exhaust) $m/z$ 44 contributes only to a small
15   degree, compared to other peaks. The ion series $m/z$ 27, 29, 41, 43, 55, 57, 69, 71, 83, 85... are representative for hydrocarbon-like organic aerosol (HOA) from fossil fuel combustion sources (Canagaratna et al., 2004; McLafferty and Turecek, 1992; Zhang et al., 2005a; Zhang et al., 2005c). The air masses that arrived from the Po valley are more influenced by fresh anthropogenic emissions than the air masses arriving
20   from the west. Interestingly, in the mass spectrum displayed in panel b) also $m/z$ 29 is a very large peak, a finding that can not be explained at the present state. The smaller relative contribution of m/z 44 to total organics is also revealed in the lower slope of the "Po Valley data" in Fig. 7. In general, the relatively small contribution of HOA in the HAZE2002 mass spectrum indicates that the ambient aerosol in the
25   Hohenpeissenberg area was not dominated by fresh anthropogenic emissions but by local biogenic emissions during the measurement period.

### 3.4.2 Polycyclic aromatic hydrocarbons (PAHs) and proteins

Figure 9 shows the measured concentrations of polycyclic aromatic hydrocarbons (PAHs) and of proteins. PAHs are characteristic trace components of pyrogenic aerosols from fossil fuel combustion and biomass burning, whereas proteins are characteristic main components of primary biological particles. The PAH concentrations were mostly in the range of $0.2$–$0.4\,\text{ng m}^{-3}$ and exhibited only little variability, except for an increase towards the end of the measurement period which coincides with lower temperatures and may be attributable to local heating emissions. Even the elevated concentrations observed at the end of the campaign ($\sim 0.6\,\text{ng m}^{-3}$), however, were much lower than the concentration levels typically observed in the nearest metropolitan area ($1$–$5\,\text{ng m}^{-3}$, city of Munich, Schauer et al., 2004, 2003a) and in polluted urban areas around the world ($20$–$110\,\text{ng m}^{-3}$ in Mexico city, 2003; Marr et al., 2006; up to $670\,\text{ng m}^{-3}$ in Delhi, 2002/2003, Sharma et al., 2007). The low PAH concentrations ($<1\,\text{ng m}^{-3}$) are fully consistent with the low EC concentrations ($<1\,\mu\text{g m}^{-3}$, Fig. 1) observed during HAZE2002; the mass fractions of PAH in diesel soot and the ratio of PAH to EC in atmospheric aerosol samples recently determined with the same analytical techniques were also on the order of $10^{-3}$ to $10^{-4}$ (Schauer et al., 2004, 2003a). Both the PAH and EC measurement results indicate a low contribution of soot and other combustion emissions to the rural aerosols sampled during HAZE2002.

The measured protein concentrations varied in the range of $0.1$–$0.6\,\mu\text{g m}^{-3}$ and followed essentially the same temporal pattern as the concentrations of PM2.5 and OM1, with pronounced minima on 20–21 and 26–29 May. The ratios of proteins to OM1 and PM2.5 were fairly constant at $\sim 8\%$ and $\sim 3\%$, respectively, indicating a substantial contribution of primary biogenic particles to the sampled rural aerosol. The relative abundance of proteins in biomass is typically on the order of $\sim 10\%$, suggesting that $\sim 30\%$ of the rural PM2.5 sampled during HAZE2002 were of primary biological origin. This first-order estimate is subject to high uncertainties with regard to the characteristic relative abundance of proteins in primary biogenic aerosol particles ($\sim 1\%$ for wood,

Title Page

Abstract | Introduction

Conclusions | References

Tables | Figures

|◄ | ►|

◄ | ►

Back | Close

Full Screen / Esc

Printer-friendly Version

Interactive Discussion

EGU

~10% for leaves, up to ~50% for microorganisms) and potential interferences of humic or humic-like substances with the determination of proteins (Fehrenbach, 2006; Franze, 2004; Ivleva et al., 2007). Thus further chemical and biological speciation will be required to corroborate these findings. Nevertheless, they are in agreement with
5  other recent studies indicating high abundances of primary biological particles in atmospheric aerosols (Despres et al., 2007; Elbert et al., 2006; Jaenicke, 2005; Poschl, 2005) and references therein. Due to the high proportion of oxygenated organic compounds typically contained in biomass, primary biological particles are likely to be detected as OOA by the AMS. Clearly, the identification of mass spectrometric markers for
10 primary biological materials appears desirable and crucial for to extend the application of AMS measurements for source apportionment of organic aerosol components.

### 3.4.3  Dicarboxylic acids and monoterpenes

Highly time resolved filter samples were taken between 22 May 2002, 06:00 and 24 May 2002, 03:00. These samples were analyzed for dicarboxylic acids originating from
15 the oxidation of monoterpenes,. At the same time gas-phase concentrations of several monoterpenes ($\alpha$-pinene, $\beta$-pinene, 3-carene and limonene) were measured online/in-situ. These data are depicted in Fig. 10, along with the aerosol mass concentrations measured by the Q-AMS as well as $O_3$ and OH gas-phase concentrations.

  The gas-phase monoterpene concentrations show a sharp decrease during the night
20 between 22 May 2002, 22:30, and 23 May 2002, 04:30. This time period is shaded grey in all four panels. Sabinic and ketolimonic acid also show a minimum during this period. The total organic aerosol as measured by the AMS does not show this minimum. We explain this sharp nighttime decrease of the monoterpenes by the meteorological situation at Hohenpeissenberg (Fig. 11): the measurement station is located on the top of a
25 small mountain that rises about 300 m above the surrounding area. During the night a stable layer is formed in the lower troposphere due to cooling of the ground. Therefore vertical mixing is very low and the station on top of Hohenpeissenberg is isolated from the emission sources (e.g., monoterpene emitting trees) on the ground. Above this sta-

ble inversion layer, wind speeds are higher and air masses are transported horizontally. Consequently the night samples are not affected by local emissions around the sampling station but represent long-range transport of air masses. Any monoterpenes that might have been present in these air masses have already reacted with the remaining

5  ozone. Gas-phase concentrations of ozone and nitrogen oxides were still present at levels comparable to those during the day (ozone remained constant at around 60 ppb). The same is true for the longer-lived aerosol species such as ammonium sulfate, ammonium nitrate, and for the concentrations of pinic and pinonic acid. The decrease of ketolimonic and sabinic acid during the night is consistent with a decrease in total

10  organics from AMS. It might be due to lower biogenic impact and lower emissions of the corresponding monoterpenes in the source area of the "aged" air mass. The atmospheric lifetimes of the dicarboxylic acids originating from terpene oxidation should be comparable. These compounds are assumed to be relatively stable and are removed from the atmosphere primarily by dry and wet deposition which should be very similar

15  for the different compounds. Using the measured $\alpha$-pinene and ozone concentrations, and yields determined in laboratory experiments, one would expect substantially higher cumulative production than observed in the aerosol. However, little is known about the decay of these compounds in the particulate phase, which may be the reason for the different behavior of the caboxylic acids displayed in Fig. 10.

20  3.5  New particle formation

An additional objective of the HAZE2002 project was the investigation of new particle formation or nucleation events. Panel c) of Fig. 1 reveals that new particle formation occurred almost regularly every afternoon, with pronounced nucleation events on 18 May 2002 and 21 May 2002. Figure 12 and Fig. 13 show the parameters relevant to

25  nucleation, measured on 18 May 2002 and 21 May 2002, respectively. Panels a) show the time series of number size distribution, measured with the SMPS in a size range between 7 and 300 nm. On 18 May 2002, the background concentration of particles in a diameter range between 10 and 100 nm before the onset of nucleation is markedly

higher than on 21 May. On both days, newly formed particles with diameters around 20–30 nm are detected in the SMPS system around 11:30. The growth of the particles in the course of the afternoon is only observed on 21 May . The particles grow in diameter from 25 nm at 11:30 until the modal diameter reaches 50 nm around 20:00 and remains stable after sunset. On 18 May the SMPS did not show the peak detected by the CPC's around 09:30 (panel b), pointing towards particle diameters below the lower cut-off size of the SMPS. Assuming particles with smaller diameter than 7 nm at 09:30 and particle growth to 20 nm at 13:00, this corresponds to growth rates of about 4 nm/h comparable to 3 nm/h on 21 May which agrees well with previous findings (Birmili et al., 2003).

Panels b) in Fig. 12 and Fig. 13 show the particle concentrations in different size ranges: The total particle concentration $N_{\text{tot}}$ (all particles with diameter >3 nm), and the ultrafine particle concentration $N_{3-14}$ (size range 3–14 nm). The ultrafine particle concentration on 18 May increases from 1780 cm$^{-3}$ at 07:44 to a maximum value of 10 990 cm$^{-3}$ at 09:55, while on 21/05, $N_{3-14}$ increases from 340 cm$^{-3}$ at 07:53 to 7100 cm$^{-3}$ at 10:55. Panels c) of Fig. 12 and Fig. 13 show the $H_2SO_4$ and OH concentrations on both days, as measured with selected ion chemical ionization mass spectrometry (SI/CIMS) (Berresheim et al., 2000). On 18 May, a maximum $H_2SO_4$ concentration of $1.9 \times 10^7$ cm$^{-3}$ is reached, on 21/05, $H_2SO_4$ reached up to $6 \times 10^6$ cm$^{-3}$. As shown in Panels d), the daytime hours featured intense solar radiation of up to 6 and 6.6 J m$^2$, temperatures up to 34°C and 25°C, and relative humidities of 50 and 70%, respectively. As additional information, the aerosol mass concentrations for organics, nitrate, sulfate, and ammonium measured on 21 May are displayed in Panel e) of Fig. 13.

Numerous observations of nucleation rates and $H_2SO_4$ vapor concentration suggest the involvement of $H_2SO_4$ in atmospheric nucleation (Kulmala et al., 2004). As a result of its low vapor pressure, sulfuric acid in the atmosphere either forms new particles through gas-to-particle conversion (Birmili et al., 2000) or condenses on pre-existing particles. The competition between these two processes is dependent on the ambient

Title Page

Abstract | Introduction

Conclusions | References

Tables | Figures

|◄ | ►|

◄ | ►

Back | Close

Full Screen / Esc

Printer-friendly Version

Interactive Discussion

EGU

aerosol size distribution and the sulfuric acid formation rate. Under the presence of gas-phase ammonia, ternary $H_2SO_4$-$H_2O$-$NH_3$ nucleation is the preferred nucleation mechanism (Korhonen et al., 1999).

Birmili et al. (2000) estimated that for ternary particle formation in the Hohenpeissenberg environment a relative atmospheric abundance of $H_2SO_4$ of at least $\sim 10^7$ cm$^{-3}$ is required. On 18 May 2002, the $H_2SO_4$ concentrations reached up to $1.9 \times 10^7$ cm$^3$ and coincided with high ultra fine particle concentrations of up to $1.1 \times 10^4$ cm$^{-3}$. On 21 May 2002, $H_2SO_4$ concentrations reached up to $6 \times 10^6$ cm$^{-3}$. These findings suggest that the observed new particle formation was due to ternary $H_2SO_4$-$H_2O$-$NH_3$ nucleation. To verify this assumption, the particle formation rate of particles between 3 and 14 nm, $J_{3-14}$, was estimated by dividing the number increase of particles between 3 and 14 nm by its corresponding duration. From the values obtained above from Panel b) in Fig. 12 we infer an average rate $J_{3-14}$ of $\sim 1.2$ cm$^3$s$^1$ for the nucleation event on 18 May 2002, and from Panel b) in Fig. 13 a rate of $\sim 0.6$ cm$^{-3}$ s$^{-1}$ for 21 May 2002. (Korhonen et al., 1999) presented calculations for the ternary $H_2SO_4$/$H_2O$/$NH_3$ nucleation from which we can infer that at an $H_2SO_4$ concentration of $6 \times 10^6$ cm$^{-3}$ and a temperature of 298 K, significant nucleation can be expected for $NH_3$ concentrations above 40 ppt. The ambient $NH_3$concentration at the Hohenpeissenberg area certainly exceeds this value (see Sect. 3.3). Thus, the observed nucleation events during HAZE2002 are very likely due to ternary nucleation which is in agreement with previous observations at Hohenpeissenberg by (Birmili et al., 2003). The aerosol mass concentrations measured by the Q-AMS on 21 May 2002 (Fig. 13, Panel e) show an increase of all species between 11:00 and 14:00. This finding suggests that not only the species that trigger the nucleation ($H_2SO_4$, $NH_3$), but also all other condensable species are involved in the particle growth, especially low-volatile organic substances.

# 4   Summary and conclusion

Microphysical properties and chemical composition of rural continental aerosol particles have been measured during HAZE2002 with a wide range of instrumentation. The data yielded size-resolved information on the chemical composition of the aerosol phase in a rural, agricultural region in Western Europe. Comparison between gravimetrically determined PM2.5 and mass spectrometrically determined non-refractory PM1 showed that on average 62% of PM2.5 was non-refractory PM1 material. The non-refractory $PM_1$ was composed to 50% of organic and 50% of inorganic components. The rural continental organic aerosol was identified as being composed mainly of oxygenated, presumably photochemically aged aerosol from both the comparison of OM1 and OC2.5 (ratio: 2.07) as well as from the mass spectrometric composition. The abundance of a mass spectrometric marker for organic aerosol from secondary sources like photochemical oxidation (m/z 44) was clearly pronounced in the afternoon due to photochemical production of low-volatile organics which condensed on pre existing particles, whereas the mass fragment 57 (marker for organic aerosol particles from primary sources like combustion) showed almost no diurnal pattern. Additionally the regression slope of the correlation between the mass concentration of the mass fragment 44 and the total organics mass concentrations indicated, that the organic compounds, measured at the Hohenpeissenberg were composed of a relatively low "base" amount of hydrocarbon-like organic aerosol (HOA) with an dominating, time-dependent contribution of oxygenated organic aerosol (OOA) that was formed during the daylight hours by photochemical processes or possibly also by downward-mixing of free tropospheric aerosol into the boundary layer. The high abundance of proteins (∼3%) indicated a high proportion of primary biological material (∼30%) in PM2.5. The low abundance of PAHs ($<1\,\mathrm{ng\,m^{-3}}$) and EC ($<1\,\mathrm{\mu g\,m^{-3}}$) in PM2.5 confirmed the low contribution of combustion emissions, which are usually also major sources for HOA. The influence of polluted air masses originating from the Po Valley, Italy, was clearly detectable during an episode and was confirmed by trajectory calculations.

Although the relative amount of inorganic aerosol components is the non-refractory PM1 remained fairly constant at 50%, the partitioning of the inorganics showed a strong dependence on temperature: At high temperatures most of the ammonium nitrate was in the gas phase, at lower temperatures more ammonium nitrate was found in the particulate phase. The decrease of the measured ammonium nitrate mass concentration with increasing temperature was described with a simple thermodynamic calculation.

New particle formation events were observed during HAZE2002 (18 May 2002 and 21 May 2002). During these nucleation events particle number densities exceeding $10^4$ cm$^{-3}$ in the nucleation mode (3–14 nm) were observed along with high sulfuric acid concentrations ($\sim 6 \times 10^6$ cm$^{-3}$). The observed particle formation rates and sulfuric acid concentrations and the estimated abundance of $NH_3$ are in agreement with calculated nucleation threshold for ternary nucleation and are also consistent with a previous long-term study and calculations.

The comparison between the mass size distribution measured with the Q-AMS and the mass size distributions inferred from SMPS and OPC data showed good agreement if the density inferred from the chemical composition was used to convert volume into mass and vacuum aerodynamic diameter into volume equivalent diameter. The refractive index of the aerosol particle was found to be around 1.40–1.45. Wet removal of aerosol particles were investigated during a precipitation event. It was found that ammonium nitrate is most efficiently removed, while organics compounds were less efficiently removed, especially small organic particles.

Summarizing, it was found that the rural continental aerosol in spring 2002 at Hohenpeissenberg was very little influenced by fresh emissions, but mainly dominated by regional and log range transport. The organic aerosol compounds were highly oxidized (OOA to HOA ratio of 4:1), and contained around 30% primary biological material. Natural aerosol sources appear to play a major role in rural continental aerosol not only in the supermicron but also in the submicron size range Since the measurement station was isolated from ground based sources due to a stable inversion layer during night time, it can be concluded that these natural sources are important not only on a local

but also on a regional scale.

## References

Alfarra, M. R., Coe, H., Allan, J. D., Bower, K. N., Boudries, H., Canagaratna, M. R., Jimenez, J. L., Jayne, J. T., Garforth, A. A., Li, S. M., and Worsnop, D. R.: Characterization of urban and rural organic particulate in the lower Fraser valley using two aerodyne aerosol mass spectrometers, Atmos. Environ., 38, 5745–5758, 2004.

Allan, J. D., Bower, K. N., Coe, H., Boudries, H., Jayne, J. T., Canagaratna, M. R., Millet, D. B., Goldstein, A. H., Quinn, P. K., Weber, R. J., and Worsnop, D. R.: Submicron aerosol composition at Trinidad Head, California, during ITCT 2K2: Its relationship with gas phase volatile organic carbon and assessment of instrument performance, J. Geophys. Res.-Atmos., 109, D13S24, doi:10.1029/2003JD004208, 2004.

Allan, J. D., Jimenez, J. L., Williams, P. I., Alfarra, M. R., Bower, K. N., Jayne, J. T., Coe, H., and Worsnop, D. R.: Quantitative sampling using an Aerodyne aerosol mass spectrometer – 1. Techniques of data interpretation and error analysis, J. Geophys. Res.-Atmos., 108, 4090, doi:10.1029/2002JD002358, 2003.

Allen, A. G., Harrison, R. M., and Wake, M. T.: A meso-scale study of the behavior of atmospheric ammonia and ammonium, Atmos. Environ., 22, 1347–1353, 1988.

Berndt, T., Boge, O., Stratmann, F., Heintzenberg, J., and Kulmala, M.: Rapid formation of sulfuric acid particles at near-atmospheric conditions, Science, 307, 698–700, 2005.

Berresheim, H., Elste, T., Plass-Dulmer, C., Eisele, F. L., and Tanner, D. J.: Chemical ionization mass spectrometer for long-term measurements of atmospheric OH and H2SO4, International Journal of Mass Spectrometry, 202, 91–109, 2000.

**Hohenpeissenberg Aerosol Characterization Experiment 2002**

N. Hock et al.

Birmili, W., Berresheim, H., Plass-Dulmer, C., Elste, T., Gilge, S., Wiedensohler, A., and Uhrner, U.: The Hohenpeissenberg aerosol formation experiment (HAFEX): a long-term study including size-resolved aerosol, H2SO4, OH, and monoterpenes measurements, Atmos. Chem. Phys., 3, 361–376, 2003,

5    http://www.atmos-chem-phys.net/3/361/2003/.

Birmili, W., Wiedensohler, A., Plass-Dulmer, C., and Berresheim, H.: Evolution of newly formed aerosol particles in the continental boundary layer: A case study including OH and H2SO4 measurements, Geophys. Res. Lett., 27, 2205–2208, 2000.

Bohren, C. F. and Huffmann, D. R.: Absorption and scattering of light by small particles, Wiley

10   and Sons, New York, 1983.

Bonn, B. and Moortgat, G. K.: New particle formation during alpha- and beta-pinene oxidation by O-3, OH and NO3, and the influence of water vapour: particle size distribution studies, Atmos. Chem. Phys., 2, 183–196, 2002,

http://www.atmos-chem-phys.net/2/183/2002/.

15   Bonn, B. and Moortgat, G. K.: Sesquiterpene ozonolysis: Origin of atmospheric new particle formation from biogenic hydrocarbons, Geophys. Res. Lett., 30, 1585, doi:10.1029/2003GL017000, 2003.

Cadle, S. H., Countess, R. J., and Kelly, N. A.: NITRIC-ACID AND AMMONIA IN URBAN AND RURAL LOCATIONS, Atmos. Environ., 16, 2501–2506, 1982.

20   Canagaratna, M. R., Jayne, J. T., Ghertner, D. A., Herndon, S., Shi, Q., Jimenez, J. L., Silva, P. J., Williams, P., Lanni, T., Drewnick, F., Demerjian, K. L., Kolb, C. E., and Worsnop, D. R.: Chase studies of particulate emissions from in-use New York City vehicles, Aerosol Science and Technology, 38, 555–573, 2004.

Canagaratna, M. R., Jayne, J. T., Jimenez, J. L., Allan, J. D., Alfarra, M. R., Zhang, Q., Onasch,

25   T. B., Drewnick, F., Coe, H., Middlebrook, A., Delia, A., Williams, L. R., Trimborn, A. M., Northway, M. J., DeCarlo, P. F., Kolb, C. E., Davidovits, P., and Worsnop, D. R.: Chemical and microphysical characterization of ambient aerosols with the aerodyne aerosol mass spectrometer, Mass Spectrometry Reviews, 26, 185–222, 2007.

Curtius, J.: Nucleation of atmospheric aerosol particles, Comptes Rendus Physique, 7, 1027–

30   1045, 2006.

DeCarlo, P. F., Slowik, J. G., Worsnop, D. R., Davidovits, P., and Jimenez, J. L.: Particle morphology and density characterization by combined mobility and aerodynamic diameter measurements. Part 1: Theory, Aerosol Science and Technology, 38, 1185–1205, 2004.

Title Page

Abstract | Introduction

Conclusions | References

Tables | Figures

◀ | ▶

◀ | ▶

Back | Close

Full Screen / Esc

Printer-friendly Version

Interactive Discussion

EGU

Despres, V., Nowoisky, J., Klose, M., Conrad, R., Andreae, M.O., and Pöschl, U.: Genetic analyses and diversity of primary biogenic aerosol particles in urban, rural, and high-alpine air, Biogeosci. Discuss., 4, 349–384, 2007.

Drewnick, F., Jayne, J. T., Canagaratna, M., Worsnop, D. R., and Demerjian, K. L.: Measurement of ambient aerosol composition during the PMTACS-NY 2001 using an aerosol mass spectrometer. Part II: Chemically speciated mass distributions, Aerosol Science and Technology, 38, 104–117, 2004.

Dusek, U., Frank, G. P., Hildebrandt, L., Curtius, J., Schneider, J., Walter, S., Chand, D., Drewnick, F., Hings, S., Jung, D., Borrmann, S., and Andreae, M. O.: Size matters more than chemistry for cloud-nucleating ability of aerosol particles, Science, 312, 1375–1378, 2006.

Elbert, W., Taylor, P. E., Andreae, M. O., and Poschl, U.: Contribution of funghi to primary biogenic aerosols in the atmosphere: Active discharge of spores, carbohydrates, inorganic ions by Asco- and Basidiomycota, Atmospheric Physics and Chemistry Discussions, 6, 11 317–11 355, 2006.

Fehrenbach, T.: Analyse von Aminosäuren, Proteinen und Nitroderivaten in atmosphärischen Aerosolen und in Straßenstaub. Technical University of Munich, Munich, 2006.

Finlayson-Pitts, B., and Pitts, J. N.: Atmospheric Chemistry: Fundamentals and experimental techniques, Wiley and Sons, New York, 1986.

Franze, T.: Analyse und Reaktivität von Proteinen in Atmosphärischen Aerosolen und Entwicklung neuer Immunoassays zur Messung von Nitroproteinen. Technical University of Munich, Munich, 2004.

Franze, T., Weller, M. G., Niessner, R., and Poschl, U.: Protein nitration by polluted air, Environ. Sci. Technol., 39, 1673–1678, 2005.

Fuzzi, S., Andreae, M. O., Huebert, B. J., Kulmala, M., Bond, T. C., Boy, M., Doherty, S. J., Guenther, A., Kanakidou, M., Kawamura, K., Kerminen, V. M., Lohmann, U., Russell, L. M., and Poschl, U.: Critical assessment of the current state of scientific knowledge, terminology, and research needs concerning the role of organic aerosols in the atmosphere, climate, and global change, Atmos. Chem. Phys., 6, 2017–2038, 2006, http://www.atmos-chem-phys.net/6/2017/2006/.

Hinds, W. C.: Aerosol technology - Properties, behavior, and measurement of airborne particles, Wiley and Sons, New York, 1999.

Ivleva, N. P., McKeon, U., Niessner, R., and Pöschl, U.: Raman microspectroscopic analysis

Title Page

Abstract | Introduction

Conclusions | References

Tables | Figures

◄ | ►

◄ | ►

Back | Close

Full Screen / Esc

Printer-friendly Version

Interactive Discussion

of size-resolved atmospheric aerosol particle samples collected with an ELPI: Soot, humic-like substances, and inorganic compounds, Aerosol Science and Technology, 41, 655–671, 2007.

Jaenicke, R.: Abundance of cellular material and proteins in the atmosphere, Science, 308, 73–73, 2005.

Jayne, J. T., Leard, D. C., Zhang, X. F., Davidovits, P., Smith, K. A., Kolb, C. E., and Worsnop, D. R.: Development of an aerosol mass spectrometer for size and composition analysis of submicron particles, Aerosol Science and Technology, 33, 49–70, 2000.

Jimenez, J. L., Bahreini, R., Cocker, D. R., Zhuang, H., Varutbangkul, V., Flagan, R. C., Seinfeld, J. H., O'Dowd, C. D., and Hoffmann, T.: New particle formation from photooxidation of diiodomethane (CH2I2), J. Geophys. Res.-Atmos., 108(D10), 4318, doi:10.1029/2002JD002452, 2003a.

Jimenez, J. L., Jayne, J. T., Shi, Q., Kolb, C. E., Worsnop, D. R., Yourshaw, I., Seinfeld, J. H., Flagan, R. C., Zhang, X. F., Smith, K. A., Morris, J. W., and Davidovits, P.: Ambient aerosol sampling using the Aerodyne Aerosol Mass Spectrometer, J. Geophys. Res.-Atmos., 108(D10), 8425, doi:10.1029/2001JD001213, 2003b.

Korhonen, P., Kulmala, M., Laaksonen, A., Viisanen, Y., McGraw, R., and Seinfeld, J. H.: Ternary nucleation of H2SO4, NH3, and H2O in the atmosphere, J. Geophys. Res.-Atmos., 104, 26 349–26 353, 1999.

Krupa, S. V.: Effects of atmospheric ammonia (NH3) on terrestrial vegetation: a review, Environ. Pollut., 124, 179–221, 2003.

Kulmala, M., Vehkamaki, H., Petajda, T., Dal Maso, M., Lauri, A., Kerminen, V. M., Birmili, W., and McMurry, P. H.: Formation and growth rates of ultrafine atmospheric particles: a review of observations, J. Aerosol Sci., 35, 143–176, 2004.

Lim, H. J. and Turpin, B. J.: Origins of primary and secondary organic aerosol in Atlanta: Results' of time-resolved measurements during the Atlanta supersite experiment, Environ. Sci. Technol., 36, 4489–4496, 2002.

Lohmann, U. and Feichter, J.: Global indirect aerosol effects: a review, Atmos. Chem. Phys., 5, 715–737, 2005,
http://www.atmos-chem-phys.net/5/715/2005/.

Marr, L. C., Dzepina, K., Jimenez, J. L., Reisen, F., Bethel, H. L., Arey, J., Gaffney, J. S., Marley, N. A., Molina, L. T., and Molina, M. J.: Sources and transformations of particle-bound polycyclic aromatic hydrocarbons in Mexico City, Atmos. Chem. Phys., 6, 1733–1745,

2006,
http://www.atmos-chem-phys.net/6/1733/2006/.

McLafferty, F. W., and Turecek, F.: Interpretation of mass spectra, University Science Books, Sausalito, 1992.

5  Meszaros, E., and Horvath, L.: concentration and dry deposition of atmospheric sulfur and nitrogen-compounds in Hungary, Atmos. Environ., 18, 1725–1730, 1984.

Morino, Y., Kondo, Y., Takegawa, N., Miyazaki, Y., Kita, K., Komazaki, Y., Fukuda, M., Miyakawa, T., Moteki, N., and Worsnop, D. R.: Partitioning of HNO3 and particulate nitrate over Tokyo: Effect of vertical mixing, J. Geophys. Res.-Atmos., 111, D15215,
10  doi:10.1029/2005JD006887, 2006.

Mozurkewich, M.: The dissociation-constant of ammonium-nitrate and its dependence on temperature, relative-humidity and particle-size, Atmos. Environ. Part a-General Topics, 27, 261–270, 1993.

Oberdorster, G.: Pulmonary effects of inhaled ultrafine particles, International Archives of Oc-
15  cupational and Environmental Health, 74, 1–8, 2001.

Pope, C. A., Burnett, R. T., Thun, M. J., Calle, E. E., Krewski, D., Ito, K., and Thurston, G. D.: Lung cancer, cardiopulmonary mortality, and long-term exposure to fine particulate air pollution, Jama-Journal of the American Medical Association, 287, 1132–1141, 2002.

Pope, C. A., and Dockery, D. W.: Health effects of fine particulate air pollution: Lines that
20  connect, J. Air Waste Manage. Association, 56, 709–742, 2006.

Poschl, U.: Atmospheric aerosols: Composition, transformation, climate and health effects, Angewandte Chemie-International Edition, 44, 7520–7540, 2005.

Rogge, W. F., Hildemann, L. M., Mazurek, M. A., Cass, G. R., and Simoneit, B. R. T.: Sources of fine organic aerosol. 9. Pine, oak and synthetic log combustion in residential fireplaces,
25  Environ. Sci. Technol., 32, 13–22, 1998.

Römpp, A.: Analysis of organic compounds in atmospheric aerodols by liquid chromatography-high resolution mass spectrometry (LC/MS/MS-ToF): Method development and applications. Johannes Gutenberg University, Mainz, 2003.

Schauer, C., Niessner, R., and Poschl, U.: Analysis of nitrated polycyclic aromatic hydrocarbons
30  by liquid chromatography with fluorescence and mass spectrometry detection: air particulate matter, soot, and reaction product studies, Analytical and Bioanalytical Chemistry, 378, 725–736, 2004.

Schauer, C., Niessner, R., and Poschl, U.: Polycyclic aromatic hydrocarbons in urban air par-

Title Page

Abstract | Introduction

Conclusions | References

Tables | Figures

◄ | ►

◄ | ►

Back | Close

Full Screen / Esc

Printer-friendly Version

Interactive Discussion

EGU

ticulate matter: Decadal and seasonal trends, chemical degradation, and sampling artifacts, Environ. Sci. Technol., 37, 2861–2868, 2003a.

Schauer, J. J., Mader, B. T., Deminter, J. T., Heidemann, G., Bae, M. S., Seinfeld, J. H., Flagan, R. C., Cary, R. A., Smith, D., Huebert, B. J., Bertram, T., Howell, S., Kline, J. T., Quinn, P., Bates, T., Turpin, B., Lim, H. J., Yu, J. Z., Yang, H., and Keywood, M. D.: ACE-Asia intercomparison of a thermal-optical method for the determination of particle-phase organic and elemental carbon, Environ. Sci. Technol., 37, 993–1001, 2003b.

Schneider, J., Weimer, S., Drewnick, F., Borrmann, S., Helas, G., Gwaze, P., Schmid, O., Andreae, M. O., and Kirchner, U.: Mass spectrometric analysis and aerodynamic properties of various types of combustion-related aerosol particles, Int. J. Mass Spectrometry, 258, 37–49, 2006.

Seidl, W., Brunnemann, G., Kins, E., Köhler, E., Reusswig, K., Ruoss, K., Seiler, T., and Dlugi, R.: Nitrate in the accumulation mode: Data from measurement campaigns in Eastern Germany. Nucleation and atmospheric aerosols, Pergamon Press, Oxford, 1996.

Seinfeld, J. H. and Pandis, S. N.: Atmospheric chemistry and physics, Wiley and Sons, New York, 1998.

Seinfeld, J. H., and Pankow, J. F.: Organic atmospheric particulate material, Ann. Rev. Phys. Chem., 54, 121–140, 2003.

Sharma, H., Jain, V. K., and Khan, Z. H.: Characterization and source identification of polycyclic aromatic hydrocarbons (PAHs) in the urban environment of Delhi, Chemosphere, 66, 302–310, 2007.

Stelson, A. W. and Seinfeld, J. H.: Relative-humidity and temperature-dependence of the ammonium-nitrate dissociation-constant, Atmos. Environ., 16, 983–992, 1982.

Takegawa, N., Miyazaki, Y., Kondo, Y., Komazaki, Y., Miyakawa, T., Jimenez, J. L., Jayne, J. T., Worsnop, D. R., Allan, J. D., and Weber, R. J.: Characterization of an Aerodyne Aerosol Mass Spectrometer (AMS): Intercomparison with other aerosol instruments, Aerosol Sci. Technol., 39, 760–770, 2005.

Turpin, B. J., and Lim, H. J.: Species contributions to PM2.5 mass concentrations: Revisiting common assumptions for estimating organic mass, Aerosol Sci. Technol., 35, 602–610, 2001.

Umhauer, H.: Particle-size distribution analysis by scattered-light measurements using an optically defined measuring volume, J. Aerosol Sci., 14, 765–770, 1983.

Weimer, S., Drewnick, F., Hogrefe, O., Schwab, J. J., Rhoads, K., Orsini, D., Canagaratna,

M., Worsnop, D. R., and Demerjian, K. L.: Size-selective nonrefractory ambient aerosol measurements during the Particulate Matter Technology Assessment and Characterization Study - New York 2004 Winter Intensive in New York City, J. Geophys. Res.-Atmos., 111, D18305, doi:10.1029/2006JD007215, 2006.

5  Willison, M. J., Clarke, A. G., and Zeki, E. M.: Seasonal-variation in atmospheric aerosol concentration and composition at urban and rural sites in northern england, Atmos. Environ., 19, 1081–1089, 1985.

Zhang, Q., Alfarra, M. R., Worsnop, D. R., Allan, J. D., Coe, H., Canagaratna, M. R., and Jimenez, J. L.: Deconvolution and quantification of hydrocarbon-like and oxygenated or-

10  ganic aerosols based on aerosol mass spectrometry, Environ. Sci. Technol., 39, 4938–4952, 2005a.

Zhang, Q., Canagaratna, M. R., Jayne, J. T., Worsnop, D. R., and Jimenez, J. L.: Time- and size-resolved chemical composition of submicron particles in Pittsburgh: Implications for aerosol sources and processes, J. Geophys. Res.-Atmos., 110, 19, 2005b.

15  Zhang, Q., Worsnop, D. R., Canagaratna, M. R., and Jimenez, J. L.: Hydrocarbon-like and oxygenated organic aerosols in Pittsburgh: insights into sources and processes of organic aerosols, Atmos. Chem. Phys., 5, 3289–3311, 2005c.

Zhang, X. F., Smith, K. A., Worsnop, D. R., Jimenez, J., Jayne, J. T., and Kolb, C. E.: A numerical characterization of particle beam collimation by an aerodynamic lens-nozzle system: Part I.

20  An individual lens or nozzle, Aerosol Sci. Technol., 36, 617–631, 2002.

Zhang, X. F., Smith, K. A., Worsnop, D. R., Jimenez, J. L., Jayne, J. T., Kolb, C. E., Morris, J., and Davidovits, P.: Numerical characterization of particle beam collimation: Part II – Integrated aerodynamic-lens-nozzle system, Aerosol Sci. Technol., 38, 619–638, 2004.

Zhang, Q., Jimenez, J. L., Canagaratna, M. R., et al.: Ubiquity and Dominance of Oxygenated

25  Species in Organic Aerosols in Anthropogenically – Influenced Northern Hemisphere Midlatitudes, Geophys. Res. Lett., in press, 2007

**Table 1.** Composition, mean particle density $p_{mean}$ and inferred refractive index n of the aerosol particles for the three time periods (A, B, and C) indicated in Fig. 3.

|   | Date & Time | $(NH_4)_2SO_4$ ($\mu g\,m^{-3}$) | $NH_4NO_3$ ($\mu g\,m^{-3}$) | Organics ($\mu g\,m^{-3}$) | $\rho_{mean}$ (g cm$^{-3}$) | $n$ |
|---|---|---|---|---|---|---|
| A | 24 May 2002, 13:48:00– 25 May 2002, 00:29:56 | 1.50 | 3.22 | 3.55 | 1.32 | 1.450 |
| B | 25 May 2002, 03:05:55– 25 May 2002, 15:47:47 | 1.17 | 0.90 | 3.42 | 1.19 | 1.400 |
| C | 25 May 2002, 16:47:47– 26 May 2002, 05:59:40 | 0.12 | 0.17 | 0.42 | 1.22 | 1.450 |

EGU
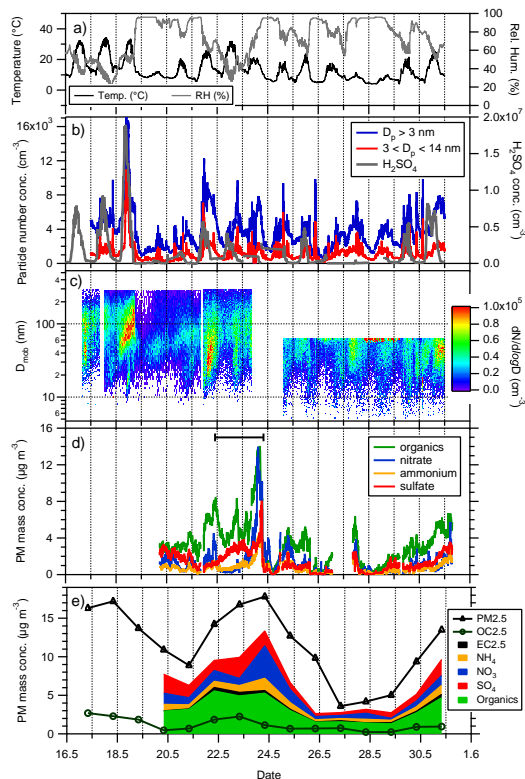
**Fig. 1.** Time series of the measured quantities during HAZE2002: **(a)** Temperature and relative humidity; **(b)** Total (>3 nm) and ultrafine (3–14 nm) particle number density along with $H_2SO_4$ number concentration. **(c)** Number size distribution measured with the SMPS; **(d)** Mass concentrations of ammonium, sulfate, nitrate and organics and measured by the QAMS; **(e)** 24-h averaged mass concentrations (stacked: organics, EC2.5, ammonium, nitrate, sulfate), along with OC2.5 and total PM2.5.

**Hohenpeissenberg Aerosol Characterization Experiment 2002**

N. Hock et al.
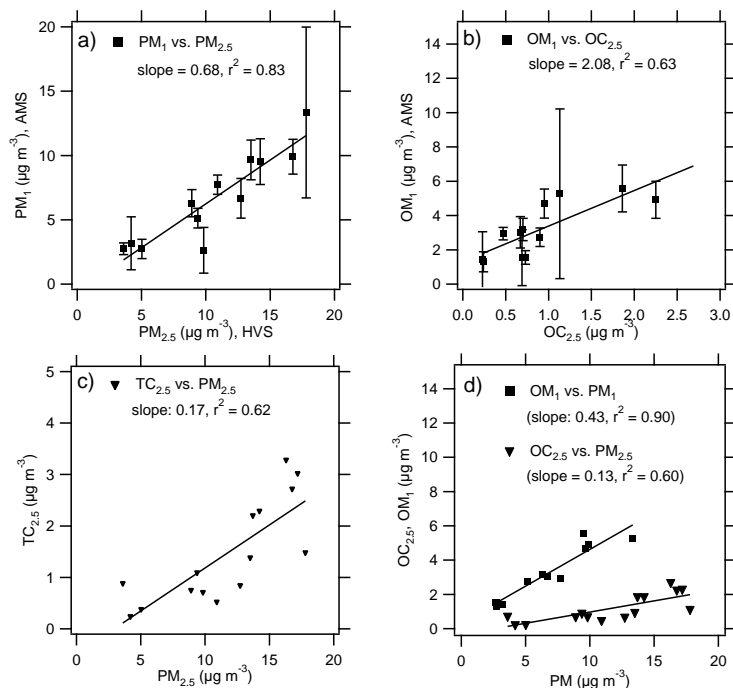
**Fig. 2.** Correlation between various aerosol parameters measured with the Q-AMS (PM1) and the HVS (PM2.5): **(a)** PM1 (derived by summing the Q-AMS mass concentrations plus EC2.5 from HVS) vs. total PM2.5 mass concentration from HVS; **(b)** Total organic mass concentration from Q-AMS (OM1) vs. OC2.5 from HVS (as difference of total carbon (TC) and elemental carbon (EC)). **(c)** Total carbon (TC2.5) vs. PM2.5 from HVS; **(d)** OM1 vs. PM1 and OC2.5 vs. PM2.5 (HVS). The error bars represent the standard deviations within the averaging intervals of Q-AMS data to HVS sampling intervals.

Title Page

Abstract | Introduction

Conclusions | References

Tables | Figures

|◄ | ►|

◄ | ►

Back | Close

Full Screen / Esc

Printer-friendly Version

Interactive Discussion

EGU
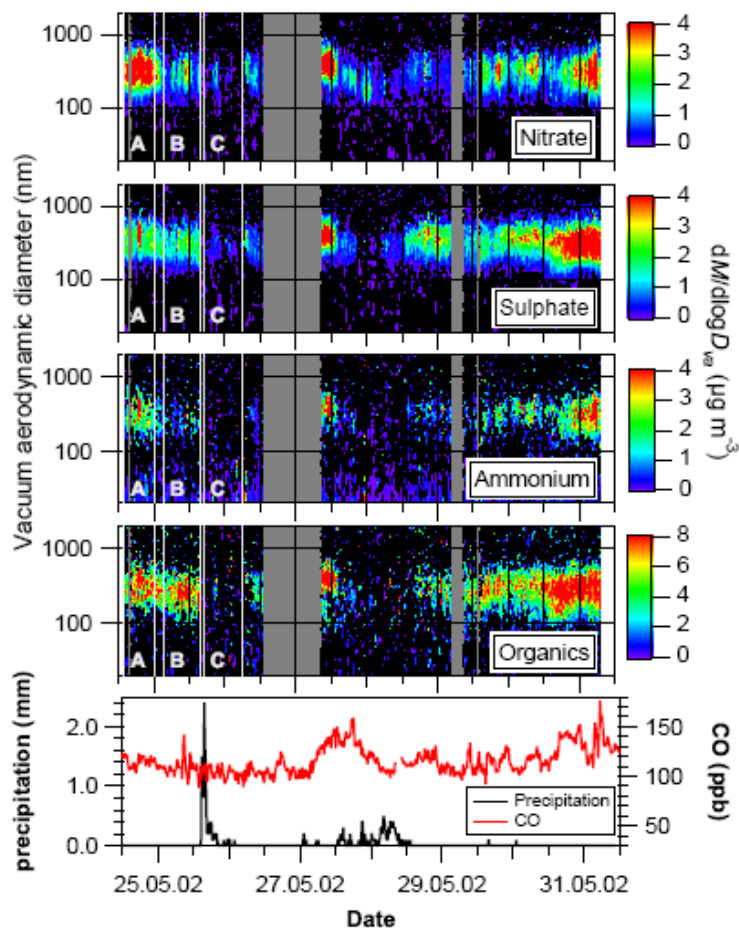
**Fig. 3.** Size distribution of the individual aerosol species measured with the Q-AMS during the second week of the campaign, along with precipitation and CO concentration.
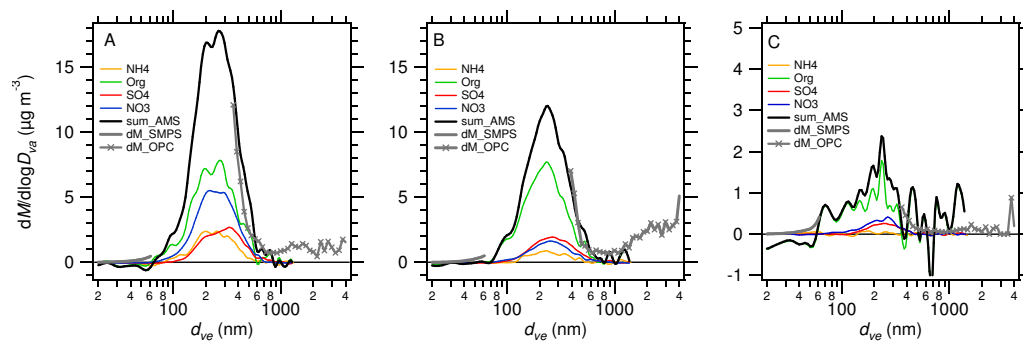
**Fig. 4.** Mass size distributions measured with the Q-AMS, SMPS and OPC for the three time periods indicated in Fig. 3.
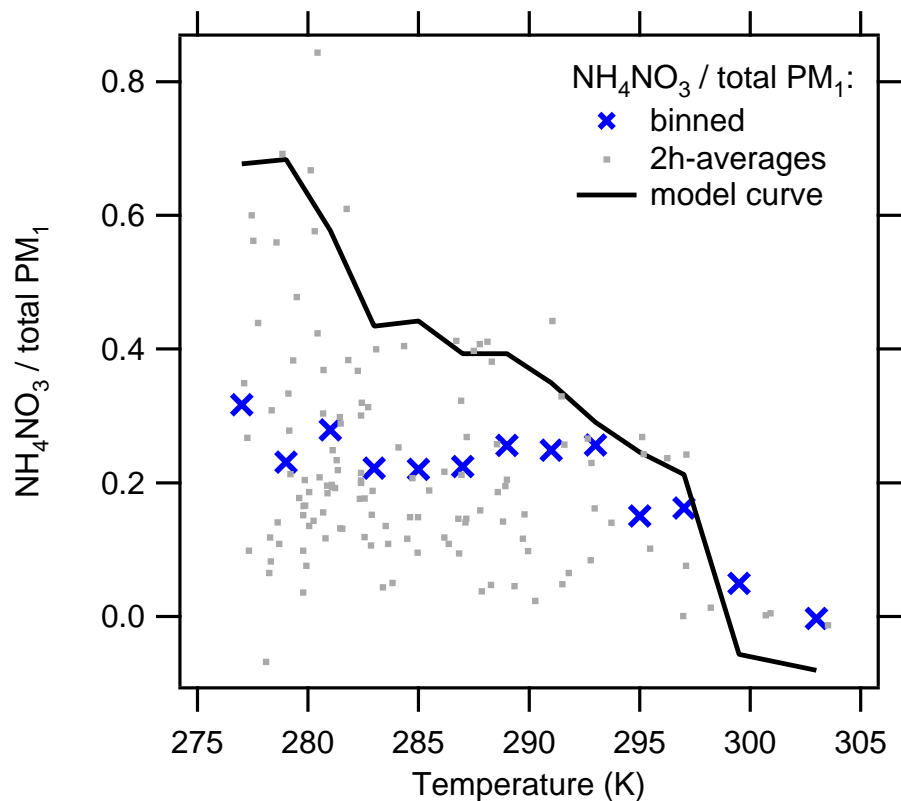
**Fig. 5.** Measured ratio of $NH_4NO_3$ mass concentration to total aerosol mass concentration as a function of temperature, binned into temperature intervals. The dots indicate the two hour averages. The solid represents a model curve with total available nitrate and ammonia as fit parameters (for details see text).
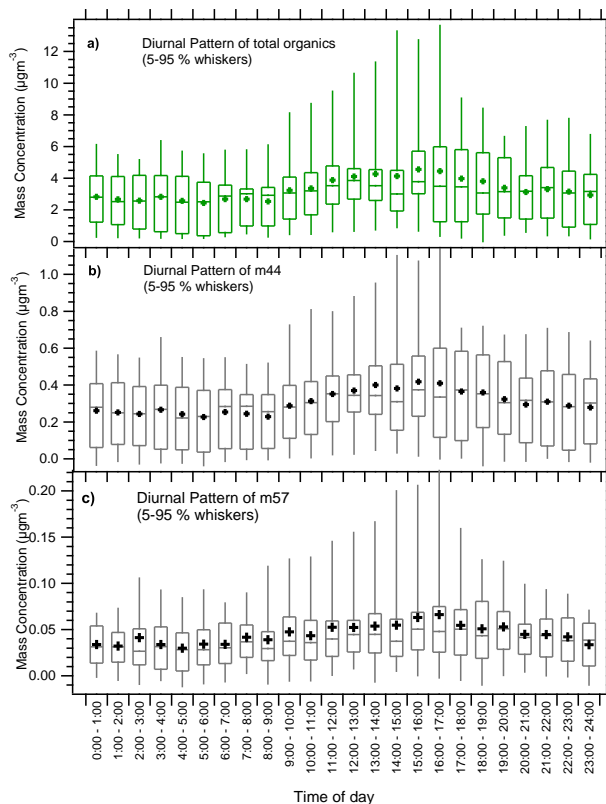
**Fig. 6.** Diurnal patterns of: **(a)** Q-AMS total organics (OM1); **(b)** m/z 44 (marker for oxygenated-like organic aerosol (OOA)); **(c)** m/z 57 (marker for hydrocarbon-like organic aerosol (HOA) from combustion sources) averaged over the whole measurement campaign. The horizontal bars indicate the median values, the boxes the 25th percentile, the median and the 75th percentile. The whiskers indicate the 5th and 95th percentile. The dots represent the mean values.
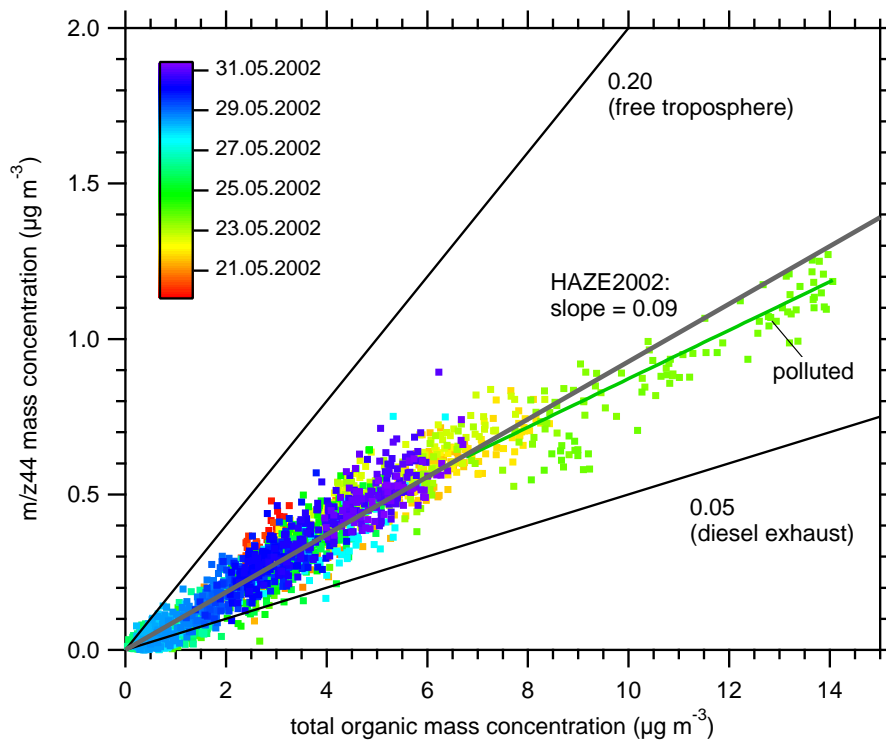
**Fig. 7.** Correlation between the mass concentrations of m/z 44 and total organics along with ratios measured in the free troposphere (Walter et al., 2007[1]) and in diesel exhaust (Schneider et al., 2006). The label "polluted" denotes only the data between 21 May 2002, 22:00 and 23 May 2002, 20:00, when the air masses originated from the Po valley.
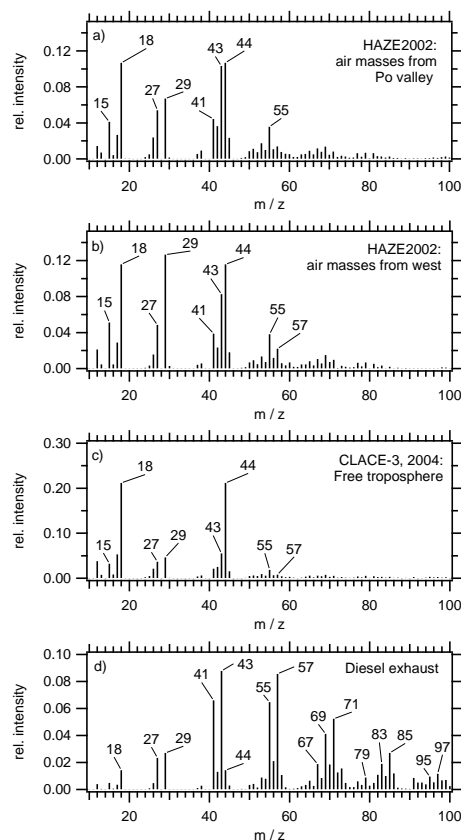
**Fig. 8.** Comparison of the mass spectra of the organic species for: **(a)** HAZE2002, averaged over the time period when the air masses arrived from the Po Valley; **(b)** HAZE2002, averaged over the time period when the air masses arrived from westerly direction; **(c)** Free tropospheric aerosol measured at the Jungfraujoch station during CLACE-3 (Walter et al., 2007[1]); **(d)** Diesel exhaust, measured at an engine test facility (Schneider et al., 2006).

EGU
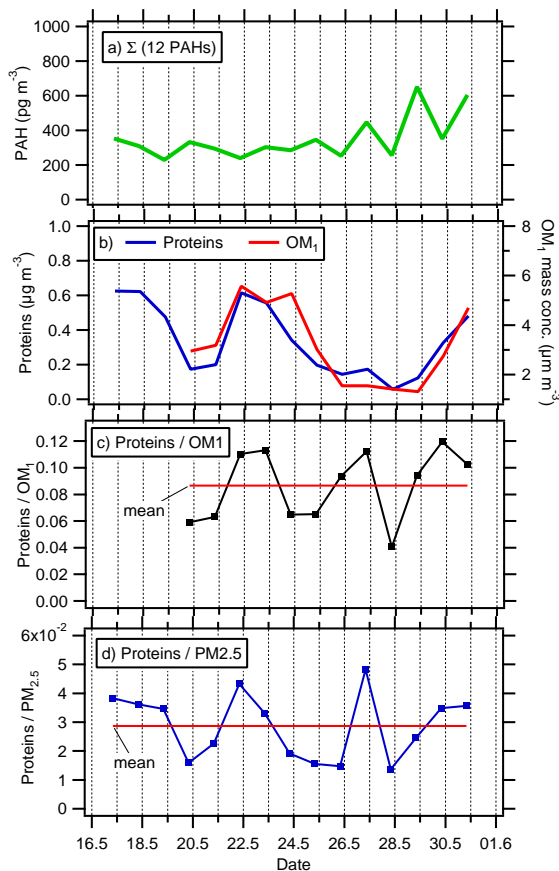
**Fig. 9.** PAHs und Proteins: **(a)** Sum of 12 PAHs; **(b)** Proteins (left scale) along with OM1 (right scale); **(c)** Ratio proteins to OM1 (mean: 0.087±0.027); **(d)** Ratio of proteins to PM2.5 (mean: 0.029±0.011).
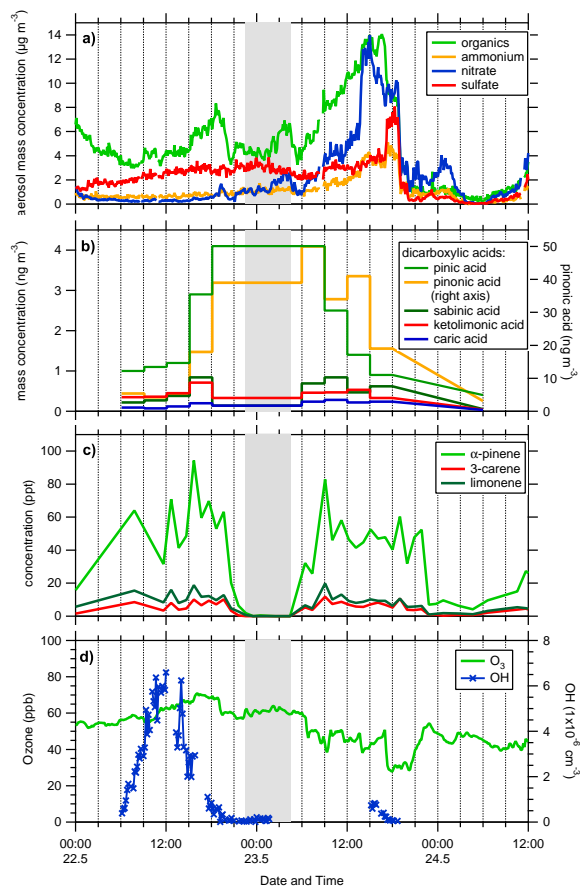
**Fig. 10.** Expanded time series 22 May to 24 May: **(a)** Non-refractory PM1 compounds (QAMS); **(b)** dicarboxylic acids; **(c)** gas-phase monoterpenes; **(d)** $O_3$ and OH.
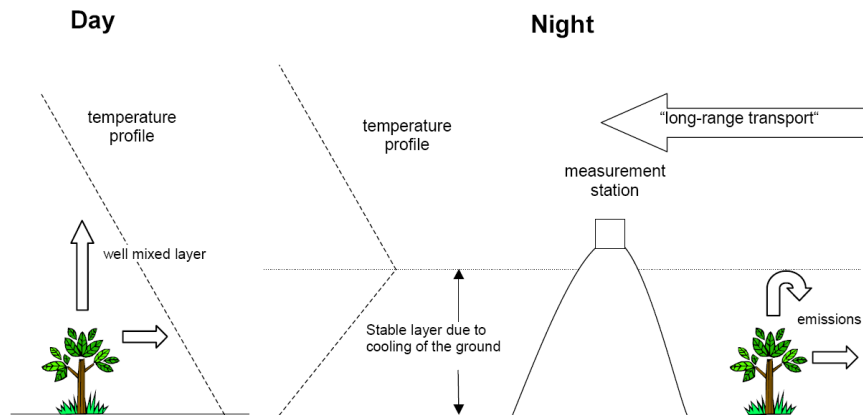
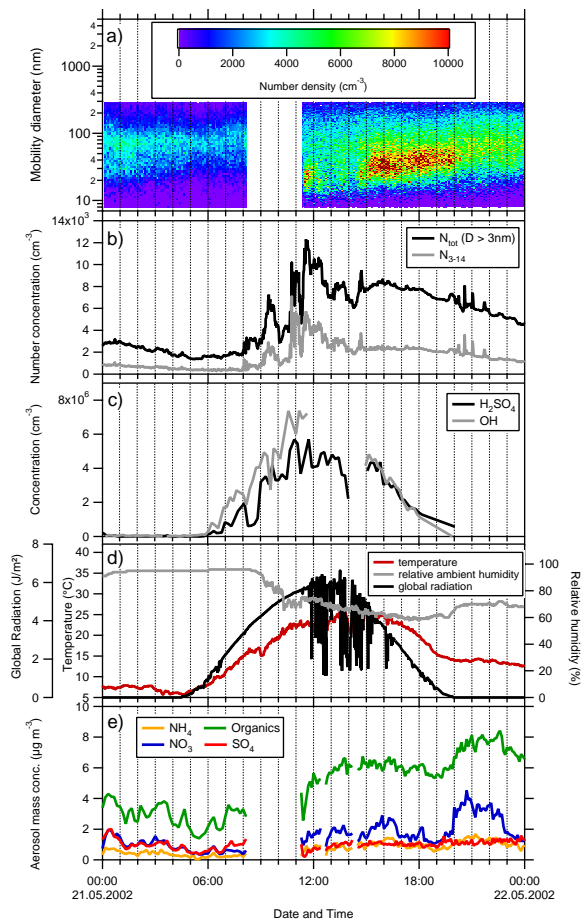**Fig. 11.** Meteorological situation at the Hohenpeissenberg.
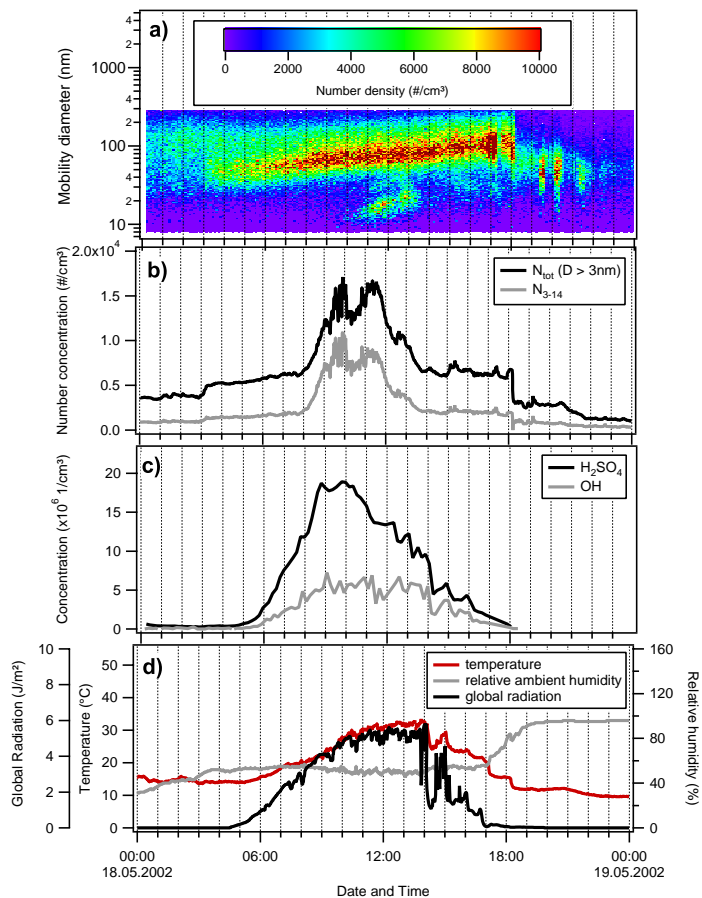
**Fig. 12.** Nucleation event on 18 May 2002. **(a)**, **(b)** Particle number density; **(c)** Gas-phase concentration of $H_2SO_4$ and OH; **(d)** Global radiation, temperature, and relative humidity.

**Fig. 13.** Nucleation event on 21/05/2002. **(a)**, **(b)** Particle number density; **(c)** Gas-phase concentration of $H_2SO_4$ and OH; d) Global radiation, temperature, and relative humidity; **(e)** Aerosol mass concentrations measured with the Q-AMS.